



Control system design for a pressure-tube-type supercritical water-cooled nuclear reactor via a higher order sliding mode method

M. Hajipour¹ · G. R. Ansarifar¹

Received: 14 February 2023 / Revised: 1 June 2023 / Accepted: 12 August 2023 / Published online: 29 January 2024

© The Author(s), under exclusive licence to China Science Publishing & Media Ltd. (Science Press), Shanghai Institute of Applied Physics, the Chinese Academy of Sciences, Chinese Nuclear Society 2024

Abstract

Nuclear power plants exhibit non-linear and time-variable dynamics. Therefore, designing a control system that sets the reactor power and forces it to follow the desired load is complicated. A supercritical water reactor (SCWR) is a fourth-generation conceptual reactor. In an SCWR, the non-linear dynamics of the reactor require a controller capable of controlling the nonlinearities. In this study, a pressure-tube-type SCWR was controlled during reactor power maneuvering with a higher order sliding mode, and the reactor outgoing steam temperature and pressure were controlled simultaneously. In an SCWR, the temperature, pressure, and power must be maintained at a setpoint (desired value) during power maneuvering. Reactor point kinetics equations with three groups of delayed neutrons were used in the simulation. Higher-order and classic sliding mode controllers were separately manufactured to control the plant and were compared with the PI controllers specified in previous studies. The controlled parameters were reactor power, steam temperature, and pressure. Notably, for these parameters, the PI controller had certain instabilities in the presence of disturbances. The classic sliding mode controller had a higher accuracy and stability; however its main drawback was the chattering phenomenon. HOSMC was highly accurate and stable and had a small computational cost. In reality, it followed the desired values without oscillations and chattering.

Keywords Supercritical water nuclear reactor · Higher order sliding mode controller · Steam temperature · Steam pressure · Point kinetics model

1 Introduction

Nuclear energy is of great interest owing to the depletion of fossil resources, pollution, greenhouse gases, and economic efficiency. Nuclear reactors are essential energy sources. The idea of fourth-generation nuclear reactors was discussed in 2002; among the six types of reactors defined by GIF, only SCWR uses supercritical water that can be either a fast or a thermal reactor. Both pressure tubes and vessels were considered for application in the SCWR. The coolant of this reactor was light water and the moderator was heavy water. The steam temperature in this reactor was strongly non-linear and highly sensitive to power disturbances [1]. One of the most critical goals in nuclear reactor control is to improve the load-following process [2–5]. In an SCWR, the

non-linear dynamics and coupling of the reactor and turbine require a controller capable of controlling these nonlinearities and couplings. Sun et al. used a strategy of changing the linear parameters to solve these problems [6]. In another study, a numerical simulation showed the stability of steam temperature in the presence of power disturbances [1]. To eliminate the coupling of the reactor and turbine, Sun et al. [2] adopted a dynamic model for a proper and safe system operation. The proportional–integral (PI) controller has been widely used in previous studies to control load following in nuclear reactors. Several methods exist for controlling a nuclear reactor; however, an efficient control system is still required because of the nonlinearity and complications of the reactor [7]. The sliding mode method involves mapping the states to a designated level known as the sliding surface. This strategy involves maintaining the proximity of the system modes in the vicinity and close proximity to the surface. Therefore, this approach is a two-part controlled method. In the first part, a sliding surface is developed according to the design specifications to accommodate the sliding motion.

✉ G. R. Ansarifar
ghr.ansarifar@ast.ui.ac.ir

¹ Department of Nuclear Engineering, Faculty of Physics, University of Isfahan, Isfahan 81746-73441, Iran

In the subsequent part, a control law is designed with the objective of assimilating the switching threshold of the states of the system. The function of the feedback control law is time-dependent. It can move from one continuous structure to another, according to the location in the state space. Consequently, the sliding mode method represents a variable structure control. In control applications, the sliding mode is commonly used as a successful approach for controlling unpredictable non-linear systems. The utilization of an SMC has been deemed a suitable technique owing to its intrinsic robustness and insensitivity to disturbances and uncertainties. This methodology possesses several notable strengths, namely, the parsimonious design, remarkable resilience in the face of various forms of interference and perturbation, capacity to effectively address model uncertainties, lower information requirements than classical control techniques, and ability to stabilize non-linear systems that are not stabilized by feedback laws. The concept of higher-order sliding modes was introduced to expand the sliding mode theory by addressing the effect of higher-order derivatives of system deviation on its suppression. Unlike conventional sliding modes that consider only the first derivative, higher-order sliding modes have been applied to novel problems. Furthermore, while concurrently retaining the primary benefits of the primary strategy, these methods eliminate chattering and allow for a more precise understanding [5]. Sliding mode controllers are commonly used to control reactors. Ansarifar et al. presented a sliding mode control approach that was gain-scheduled to regulate the water level in a reactor [8]. The advantage of the sliding mode is that it can

force the system dynamics to behave in the desired pattern with the correct choice of the sliding surface. Furthermore, the closed-loop characteristics exhibit a significant level of insensitivity toward various sources of uncertainty, including model parameters, disturbances, and nonlinearities. Nonlinear processes can be effectively controlled in the case of model disturbances and uncertainties by implementing a sliding mode methodology. The classic sliding mode controller suffers from a significant drawback, that is, high-frequency oscillations in the output signal in the steady state, known as the chattering phenomenon. To overcome this limitation, an HOSMC is employed that ensures a smooth control signal without chattering. In another study, Ansarifar et al. introduced a sliding mode controller designed for a specific PWR to enhance the capacity of the reactor to adjust to varying power loads [9]. For the first instance, the present study employed a sliding mode control methodology to regulate the supercritical water nuclear reactor system. Conventional and higher-order sliding mode controllers were employed and simulated independently to control the power output of the reactor, outgoing coolant pressure, and temperature. The results were subsequently compared with those obtained using a PI controller. The results of this study have the potential for practical application in the development of an appropriate controller for an operational system. The reactor point kinetic model was used to implement both the classic and second-order sliding mode controllers, and their ability to withstand disturbances was subsequently assessed and compared with that of the PI controller. The configuration of the reactor and turbine is shown in Fig. 1.

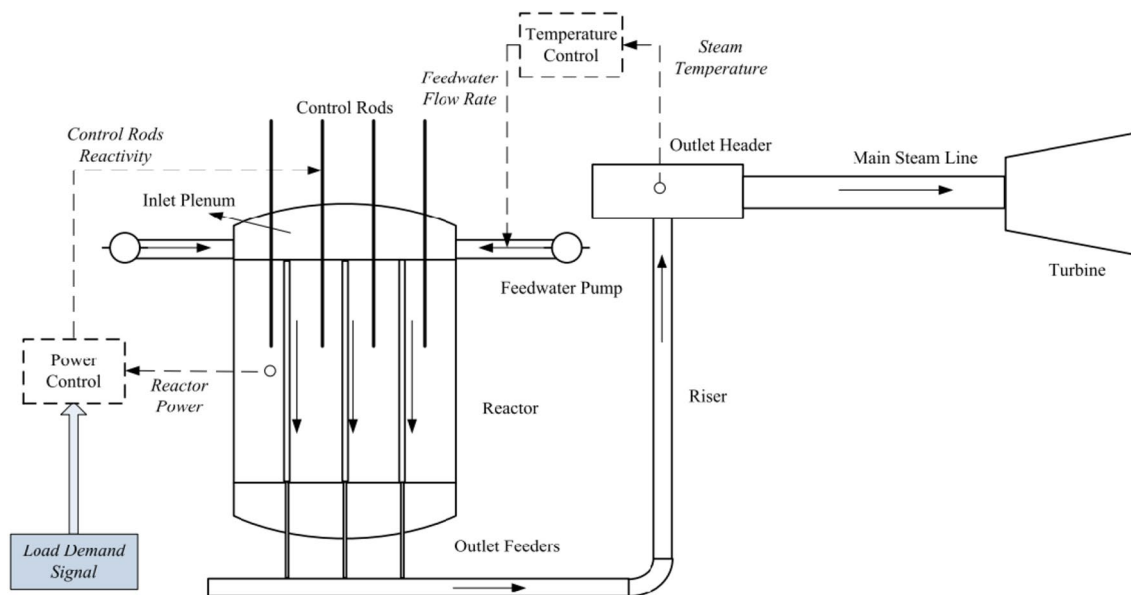


Fig. 1 Reactor and turbine model [2]

2 Materials and methods

2.1 Nuclear reactor core model

This section delves into a comprehensive investigation of the reactor model, the neutronic model of the reactor, and the thermohydraulic model of the system. The dynamic equations are derived using the principles of mass, energy, and momentum conservation [2].

$$V \frac{d\rho_0}{dt} = Q_i - Q_o \quad (1)$$

$$V \frac{d}{dt}(\rho_0 h_o) = Q_i h_i - Q_o h_o \quad (2)$$

$$\frac{dQ_o}{dt} = \frac{Q_i - Q_o}{\tau} \quad (3)$$

$$T_o = \frac{h_o - h_i}{c_p} + T_i \quad (4)$$

The present analysis considers several parameters pertaining to the steam chamber, including the inlet steam flow rate (Q_i) and outlet steam flow rate (Q_o), both expressed in units of kg/s. The specific enthalpies at the inlet (h_i) and outlet (h_o) of the reactor are reported in units of kJ/kg. Additionally, the outlet steam density (ρ_o) is presented using units of kg/m³, whereas volume (V) is expressed in units of m³. A time constant (τ) of 0.4 s is also considered. The inlet and outlet steam temperatures of the reactors (T_i and T_o , respectively) are expressed in units of K. The specific heat of steam at constant pressure (C_p) is measured in units of kJ/(kg K). The outlet steam pressure of the reactor is defined as follows:

$$P_o = R\rho_o T_o \quad (5)$$

Here, P_o represents the outlet steam pressure of the reactor (MPa), and R represents the ideal gas constant, 462 (J/kg K). Because of absence of a physical model, this model is the best option for current studies [2]. The assumed specifications of the plant are presented in Table 1.

In this study, a lumped model is employed for the fuel and coolant, and a dynamic model is formulated using point kinetic equations. The dynamic model is devised by incorporating three groups of delayed neutrons, drawing inspiration from the Skinner–Cohen model. Its accuracy is established through validation and benchmarking [4]. The normalized model for the equilibrium condition is as follows:

$$\frac{dn_r}{dt} = \frac{\rho - \beta}{l} n_r + \sum_{i=1}^3 \frac{\beta_i}{l} c_{ri}, \quad (6)$$

Table 1 Preconceptual characteristics of a Canadian SCWR [2]

Parameters	Value
Spectrum	Thermal
Moderator	Heavy water
Coolant	Light water
Thermal power (MW)	2540
Flow rate (kg/s)	1320
Efficiency	48%
Inlet temperature (°C)	350
Outlet temperature (°C)	625
Cladding temperature (°C)	< 850

$$\frac{dc_{ri}}{dt} = \lambda_i n_r - \lambda_i c_{ri}, \quad i = 1, 2, 3 \quad (7)$$

$$\frac{dT_f}{dt} = \left(\frac{1}{\mu_f} \right) (p_0 n_r - hA(T_f - T_c)), \quad (8)$$

$$\frac{dT_c}{dt} = \left(\frac{1}{\mu_c} \right) (hA(T_f - T_c) - 2Q_i C(T_c - 350)), \quad (9)$$

$$\rho = \rho_r + \alpha_f(T_f - T_{f0}) + \alpha_c(T_c - T_{c0}). \quad (10)$$

Here, n_r represents the relative neutron density, ρ represents reactivity, β represents the total delayed neutron fraction, β_i represents the i -th group delayed neutron fraction, c_{ri} represents the relative density of the i -th group precursor, l represents the prompt neutron lifetime, λ_i represents the radioactive decay constant of i -th group neutron precursor s⁻¹, T_f and T_c denote the average fuel and coolant temperature, respectively (°C), p_0 represents the initial equilibrium power (MW), h represents the heat transfer coefficient between the fuel and the coolant, A represents the heat transfer area between the fuel and the coolant, μ_f and μ_c denote the total heat capacity of the fuel and coolant, respectively (MW·s/°C), C represents the specific heat capacity of the coolant, ρ_r represents the control rod reactivity that is the output of the reactor power controller, α_f represents fuel temperature reactivity coefficient $\frac{\Delta k}{k}/^\circ\text{C}$, α_c represents coolant temperature reactivity coefficient $\frac{\Delta k}{k}/^\circ\text{C}$, T_{f0} represents the initial equilibrium (steady-state) fuel temperature, and T_{c0} represents the initial equilibrium (steady-state) coolant average temperature. In this model, the control inputs are control rods reactivity ρ_r and feedwater flow rate that is equal to the inlet steam flow rate of the reactor Q_i ; the outputs are reactor relative power that is equal to relative neutron density n_r , outlet steam temperature of the reactor T_o , and outlet steam pressure of the reactor P_o . Because pressure is a direct function of the outlet steam temperature of the reactor, as described in Eq. (5), it can be controlled via Q_i .

2.2 PI controller design

A PI controller is a control loop system that employs feedback and is widely used in industrial systems. The PI controller successively calculates an error by subtracting the actual and desired values, and produces an input signal for the next iteration from the sum of the proportion and integral of the error. Figure 2 shows a schematic of the PI controller.

In this case, two PI controllers are implemented in the system to control the reactor power, outlet steam temperature, and reactor pressure that is a direct function of its temperature. A simplified (without intermediate states of the system) MATLAB SIMULINK design for the system with PI controllers is shown in Fig. 3a. The first PI controller receives the steam temperature error as input. The controller then produces an output signal corresponding to the inlet feedwater flow rate of the reactor. The second PI controller receives as its input the difference between the measured relative power of the reactor and its setpoint value (equal to the relative neutron density) from the desired value. The output signal is the control rod reactivity. Both PI controllers are tuned using the MATLAB SIMULINK auto-tuning feature in the PI blocks. The tuned parameters for the PI controllers are listed in Table 2.

2.3 Classic sliding mode controller

Employing the sliding mode constitutes a streamlined approach to the concept of robust control. The sliding mode is the main configuration of variable structure systems. The

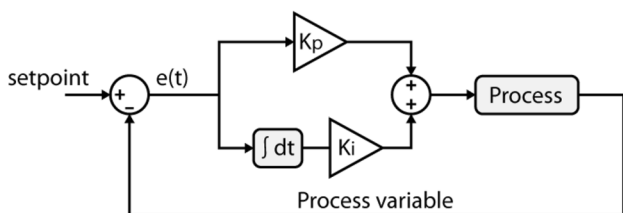


Fig. 2 PI controller model

Fig. 3 Simplified controller design for a PI, and b sliding mode

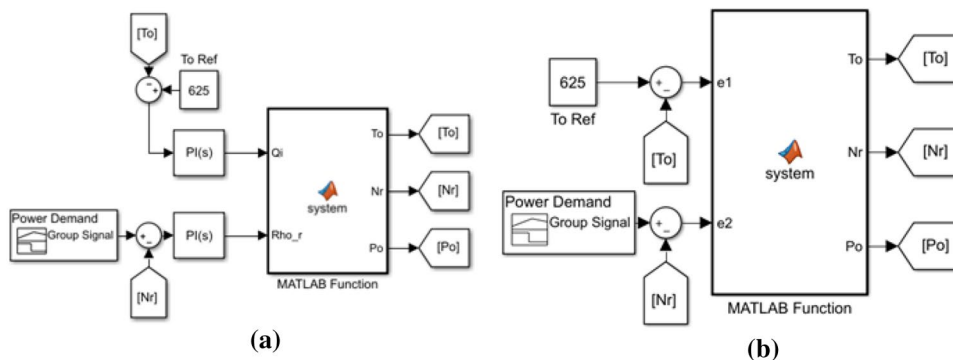


Table 2 Auto-tuned parameters for PI controllers

Controller	K_p	K_I	Overshoot (%)	Settling time (s)	Rise time
T_o	0.75	0.53	4.5	28	1.2
N_r	0.44	0.0038	3.76	19	3.57

controller design consisted of two steps: designing the sliding surface and controlling the input. In a typical non-linear system,

$$\begin{cases} \dot{x}(t) = v(x) + w(x)u \\ y = z(x) \end{cases} \quad (11)$$

Here, v , w , and z possess a satisfactory level of smoothness. Based on error $e(t) = y_d - y$, switching surface $s(t)$ is defined as follows:

$$s(t) = \left(\frac{d}{dt} + \lambda \right)^{r-1} e(t). \quad (12)$$

By solving $s(t) = 0$, a stable switching surface is obtained, where λ denotes the sliding surface coefficient presenting the bound of the error dynamics and r is a comparative degree. The control signal is defined as follows:

$$u = -K \tanh \left(\frac{s}{\varphi} \right). \quad (13)$$

Here, K represents a sufficiently large positive constant, and φ denotes the thickness of the boundary layer. A simplified (without intermediate states of the system) MATLAB SIMULINK design for the system with the first-order sliding mode controllers is shown in Fig. 3b. In this case, the controllers are designed within the system block. e_1 represents the error of T_o from the desired value, and e_2 represents the error of N_r from the desired value. Then, s_1 and s_2 are obtained using Eq. (12), and control signals u_1 and u_2 are generated by Eq. (13). These two signals are the actuator signals for the inlet feedwater flow rate that is identical to the

inlet steam flow rate of reactor Q_i and control rod reactivity ρ_r , respectively. Table 3 lists the control parameters used in this study.

2.4 Higher-order sliding mode controller

The higher-order sliding mode is a fundamental concept related to the discontinuity set of a dynamic system. The level of smoothness in the dynamics of mode proximity is ascertained by the order of sliding. To maintain the prescribed constraint that is defined by the s function being equal to zero, the sliding order is determined by the total number of derivatives of s within the sliding mode region. The formation of the r th-order sliding mode is accomplished using a set of equations [5].

$$s = \dot{s} = \ddot{s} = \dots = s^{(r-1)} = 0 \quad (14)$$

Dynamic system states coalesce to generate an r -dimensional form. A principal concern associated with the utilization of higher-order sliding modes is the escalating demand for system information. The accessibility of s , \dot{s} , \ddot{s} , and their $(r-1)$ derivatives is imperative to ensure the effective function of any controller that performs r -sliding while maintaining $s=0$. At present, the sole exception that exists pertains to the “super twisting” second-sliding controller that possesses the distinctive characteristic of solely necessitating the computation of s [5]. This algorithm converges in a limited time to the sliding pair ($s=\dot{s}=0$) and is as follows:

$$\begin{cases} u = -\gamma\sqrt{|s|}\text{sgn}(s) + w \\ \dot{w} = -W\text{sgn}(s) \end{cases} \quad (15)$$

Parameter γ determines both the degree of overshoot and the magnitude of steady-state error in a system. Increasing the magnitude of γ decreases overshoot; however, concurrently, the steady state error increases. On the contrary, by reducing the magnitude of the γ , precise tracking is attained, albeit at the expense of elevated overshoot. The speed of convergence is influenced by factor W , whereby smaller values of W result in a slow convergence of the output to its ultimate value, whereas larger values of W prompt a more

rapid convergence. This relationship between W and the convergence rate of the output denotes an essential aspect in the analysis of the system under consideration.

A convenient method to set the parameters of this control law is as follows:

$$\begin{cases} \gamma = \sqrt{K} \\ W = 1.1K \end{cases} \quad (16)$$

In practice, K can be gradually increased to achieve the proper closed-loop system performance. System parameters or sliding variables are not required in this algorithm [10]. In this particular scenario, parameters s_1 and s_2 are derived by applying the first-order sliding mode methodology. Upon obtaining these values, control signals u_1 and u_2 are produced using Eq. (15). Similar to the previous case, these two signals are actuator signals for Q_i and ρ_r , respectively. The simplified MATLAB SIMULINK design of the system is similar to that shown in Fig. 3b. Sliding mode controllers have uncertain convergence time, implying that they only ensure the system reaches a steady state when time tends to infinity and cannot specify a certain finite value of the convergence time. Therefore, any positive constants for λ and K (in the first-order sliding mode) or λ and W (in the higher-order sliding mode) that reach a steady state in finite time are acceptable [11]. Table 3 lists the control parameters pertinent to the higher-order sliding mode.

3 Results and discussions

In this study, a performance analysis of the suggested control structures was performed using MATLAB software to simulate the system as characterized in the preceding section. The PI, classic sliding mode, and second-order sliding mode techniques were employed in the implementation of the plant. The ultimate objective in all instances was to adhere to the intended power output while ensuring that the steam temperature and pressure were maintained at their designated setpoints throughout the load-following procedure. The controlled parameters were reactor relative power n_r , outlet steam pressure of the steam chamber P_o , and outlet steam temperature of the steam chamber T_o . The reactor power was controlled by the reactivity of the control rods, whereas the steam pressure and steam temperature were adjusted by the feedwater flow rate. As shown in Eq. (5), the outlet pressure of the steam chamber is a direct function of its temperature; hence, controlling the temperature and outlet steam density of the steam chamber forces the pressure at the designed constant value. Therefore, the steam pressure and steam temperature can be controlled using the feedwater flow rate as the control input. The control inputs were control rod reactivity, ρ_r , and feedwater flow rate that

Table 3 Control parameters for FOSMC and HOSMC

Controller	λ (Sliding surface coef-ficient)	K
FOSMC		
T_o	12	110
N_r	10	115
HOSMC		
T_o	100	15
N_r	100	15

was equal to the inlet steam flow rate of the steam chamber, Q_i . The simulation entailed using a load pattern that involved a gradual increase in load from 90% full power (FP) to 100%FP at a rate of 5% per minute. The objective was to initiate power output at 100%FP for 100 s, followed by a linear reduction in output from 100%FP to 90%FP over 120 s. Subsequently, power output had to be sustained at 90%FP for 160 s, followed by a linear increase in output from 90%FP to 100%FP over 120 s. Finally, power output had to be sustained at 100%FP for an interval of 100 s. To analyze the robustness of the controller design, a pulse-type disturbance was applied to all the controllers, as depicted in Fig. 4. Figure 5a shows the performance of the PI controller, SMC, and HOSMC for desired power magnitude change at a rate of 5%FP/min in the absence of disturbance. The PI controller had an overshoot at the start, between 180 and 420 s, and the SMC did not completely follow the demand because of the chattering phenomenon and measurement noise. However, the HOSMC reached the desired level without overshoot or error. Figure 5b shows the temperature of the outlet steam chamber for the PI controller, SMC, and HOSMC. As shown in the figure, the PI controller had oscillations and did not reach the desired value at the end, the SMC had fluctuations and chattering, and HOSMC followed the desired value without fluctuations or chattering. Figure 5c shows the pressure in the outlet steam chamber for the PI controller, SMC, and HOSMC in the absence of disturbances. As shown in this figure, the PI controller had fluctuations and did not reach the desired value at the end, the SMC had fluctuations and chattering, and the HOSMC followed the desired value without fluctuations or chattering. Because the pressure is a direct function of the outlet temperature of the reactor, the temperature and pressure figures are similar at larger scales. Figure 5d shows the performances of the PI controller, SMC, and HOSMC for the desired power change with disturbance.

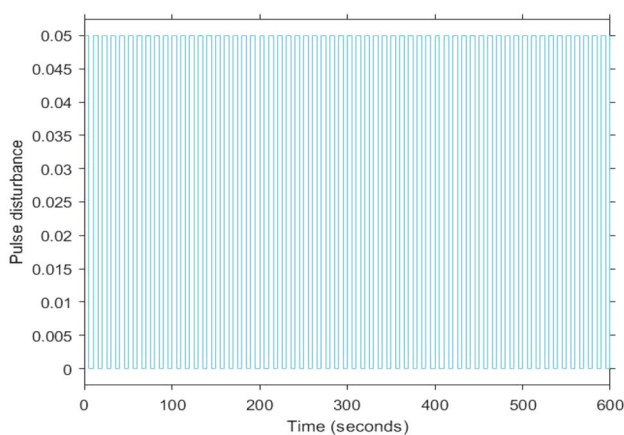


Fig. 4 Disturbance (pulse type)

The PI controller oscillated around the desired value. The SMC had an overshoot at the start, did not wholly follow the desired value, and had fluctuations. However, the HOSMC achieved power levels without overshoot, error, or shaking.

Figure 5e shows the temperature of the outlet steam chamber for the PI controller, SMC, and HOSMC in the presence of disturbance. As shown in this figure, the PI had oscillations and did not reach the desired value at the end, the SMC had fluctuations and chattering, and the HOSMC followed the desired value without fluctuations or chattering.

Figure 5f shows the pressure of the outlet steam chamber for the PI controller, SMC, and HOSMC in the presence of disturbance. As shown in this figure, the PI controller had oscillations and did not reach the desired value at the end, the SMC had an overshoot at the start and oscillations and chattering, the HOSMC followed the desired value without fluctuations or chattering. Figure 6a–c show the control rod reactivity and overall core reactivity for the PI controller, SMC, and HOSMC in the absence of disturbance, respectively. Overall reactivity began at zero and decreased after 120 s to decrease the power level, then increased to set back power to 100%FP, and then tended to drop to zero to maintain the power at 100%FP. The control rod reactivity exhibited a pattern similar to that for the power in all controllers to regulate the power according to the requested demand. Figure 6d–f show the control rod reactivity and overall core reactivity for the PI controller, SMC, and HOSMC in the presence of disturbance, respectively. These patterns were similar to those observed in the no-disturbance condition. The PI controller and SMC exhibited large oscillations, and the SMC underwent abrupt changes in the early stages because of the chattering phenomenon and measurement noise. However, the HOSMC produced a smooth signal with no fluctuations, indicating a suitable and applicable control effort for the HOSMC compared with the other methods. Figure 7a–c show the inlet feedwater flow rate of the reactor, Q_i , for the PI controller, SMC, and HOSMC, respectively, in the absence of disturbance, that is the actuator signal used to control the outlet steam temperature and pressure of the reactor. The PI controller and HOSMC reached the desired values with no overshoot or error, but the SMC exhibited oscillations at certain points. Owing to the chattering phenomenon and measurement noise, certain abrupt changes were observed, as shown in Fig. 7b. Figure 7d–f show the inlet feedwater flow rate of the steam chamber for the PI controller, SMC, and HOSMC in the presence of disturbances, respectively; they exhibited patterns similar to those for power. The PI controller and SMC exhibited large oscillations. However, the HOSMC produced a smooth signal with no fluctuations, indicating a suitable

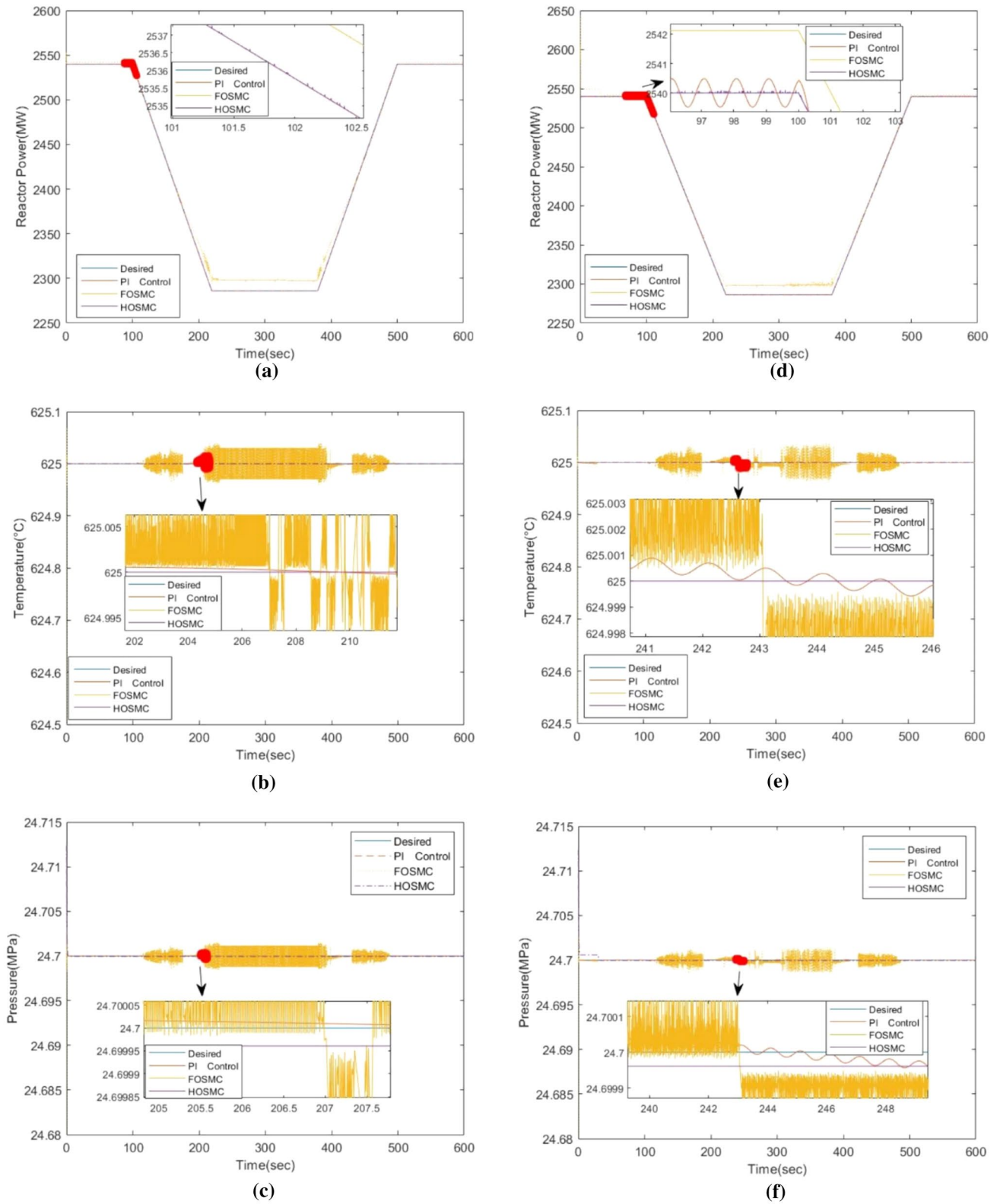
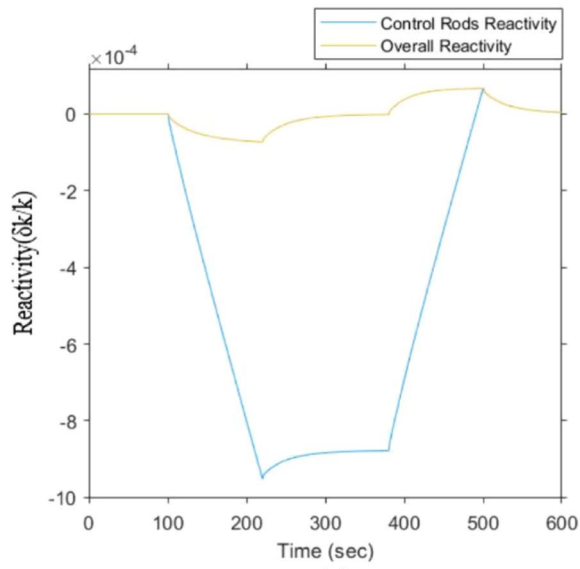
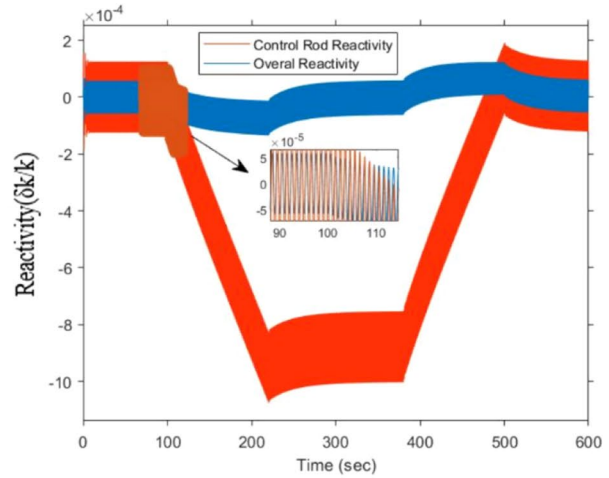


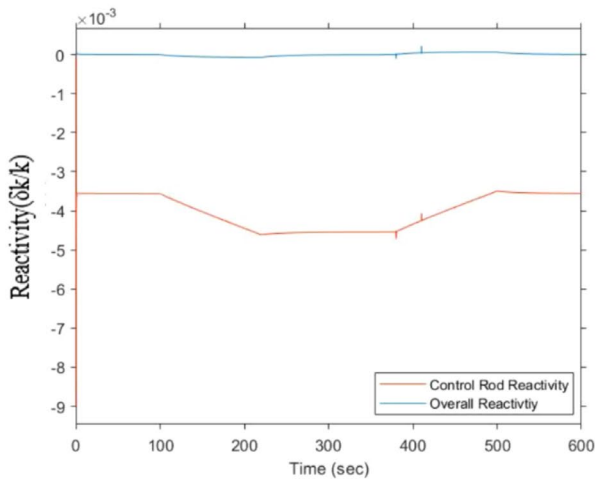
Fig. 5 (Color online) Reactor outputs. **a** Power, **b** temperature, and **c** pressure in the absence of disturbance. **d** Power, **e** temperature, and **f** pressure in the presence of disturbance



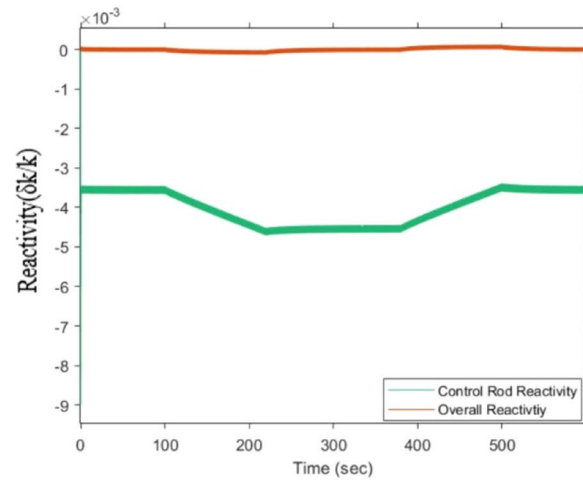
(a)



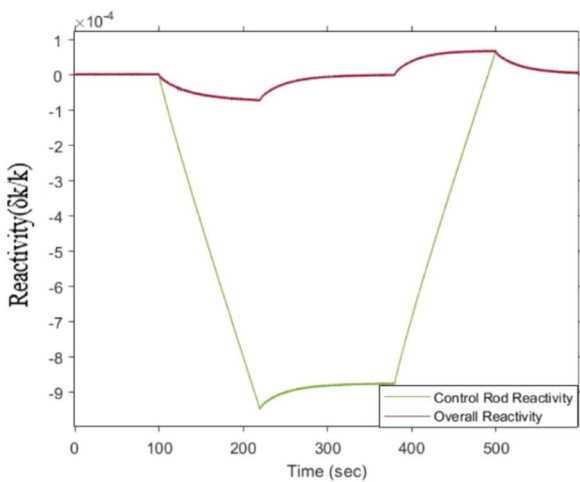
(d)



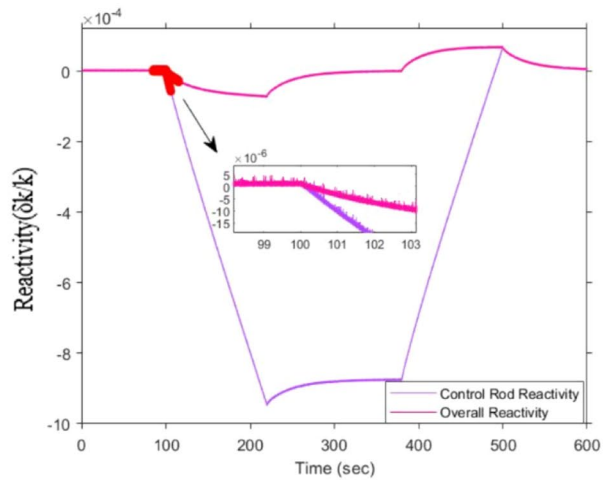
(b)



(e)



(c)



(f)

Fig. 6 (Color online) Control rod and overall reactivity. **a** PI, **b** FOSMC, and **c** HOSMC in the absence of disturbance. **d** PI, **e** FOSMC, and **f** HOSMC in the presence of disturbance

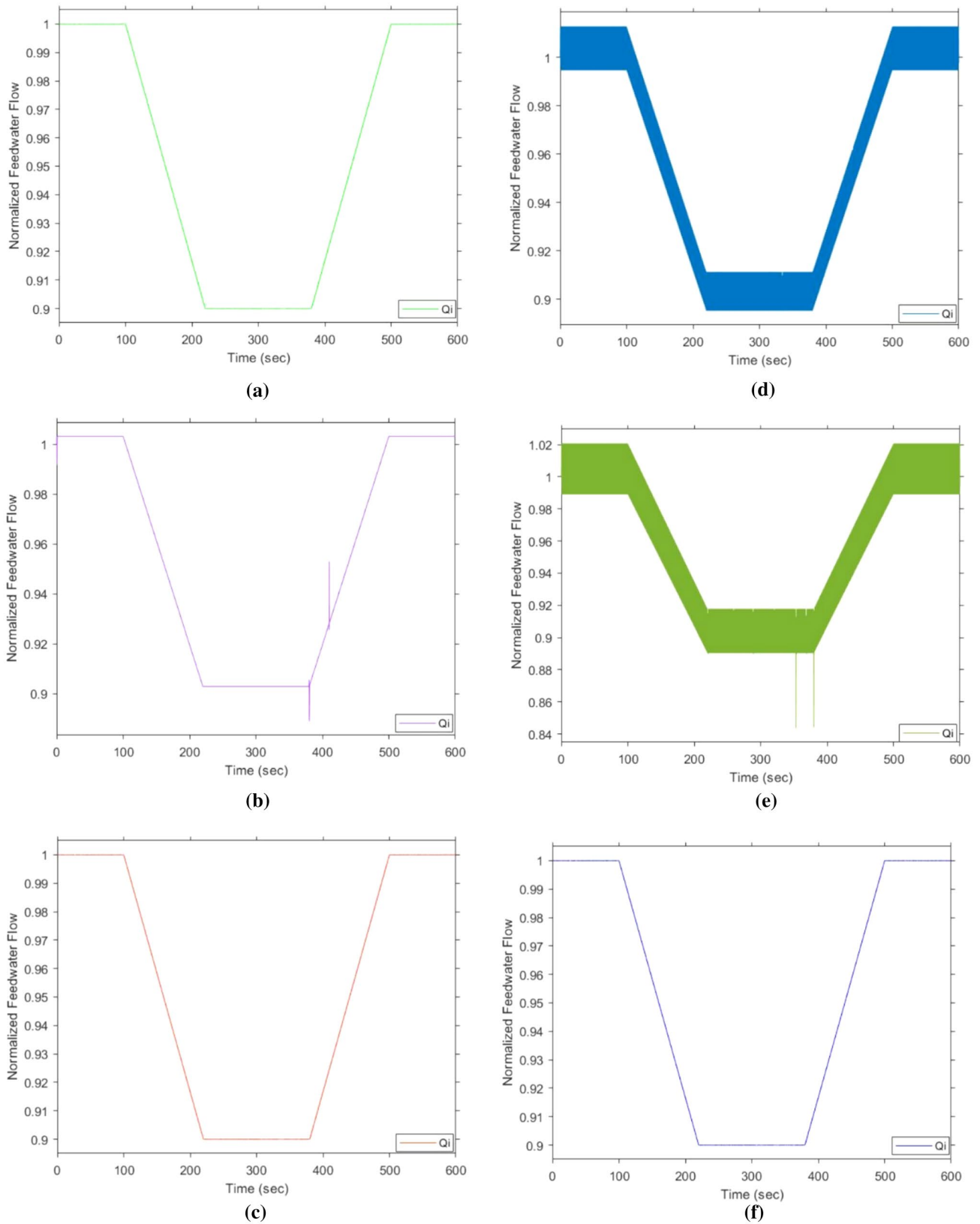


Fig. 7 (Color online) Normalized feedwater flow. **a** PI, **b** FOSMC, and **c** HOSMC in the absence of disturbance. **d** PI, **e** FOSMC, and **f** HOSMC in the presence of the disturbance

and applicable control effort for the HOSMC compared with the other methods.

4 Conclusion

This study entails the development of a higher-order sliding mode controller intended for a pressure-tube-type SCWR, wherein the reactivity feedback effects are considered during power maneuvering that can simultaneously control the reactor power, steam temperature, and steam pressure. Simulation of the reactor core was based on point kinetics equations with three groups of delayed neutrons. The thermal reactivity feedback was modeled based on the lumped coolant and fuel temperature. The inputs to the reactor power and steam temperature controllers were the steam reactor power and steam temperature differences from their setpoints, respectively. The outcome of the reactor power controller is the control rod reactivity. In addition, the production of the steam temperature controller depends on the feedwater flow rate. The PI controller, SMC, and HOSMC were implemented in a SCWR to investigate the performance of each controller. As discussed in Sect. 3, the PI controller and SMC encountered certain problems in simultaneously controlling the reactor power, outlet steam temperature, and pressure of the reactor and had large oscillations in the presence of disturbances. However, the HOSMC has high accuracy, no fluctuation or chattering, and high precision with an applied disturbance. In addition, the control rod reactivity and feedwater flow rate as control inputs exhibited acceptable behavior and smooth signals without oscillation or chattering when using the HOSMC.

The main advantages of the HOSMC are easy application in real applications, simple controller structure design, and sufficient load-following performance.

Therefore, during the output-tracking process, higher-order sliding mode control satisfies the desired dynamics and significantly improves current controller systems such as PI controllers.

References

1. P.W. Sun, J. Zhang, G. Su, Linear parameter-varying modeling and control of the steam temperature in a Canadian SCWR. *Nucl. Eng. Des.* **313**, 225–235 (2017). <https://doi.org/10.1016/j.nucengdes.2016.12.025>
2. P.W. Sun, J. Zhang, Control strategy for once-through direct cycle Canadian SCWRs. *Prog. Nucl. Energy* **98**, 202–212 (2017). <https://doi.org/10.1016/j.pnucene.2017.03.024>
3. M. Yetisir, W. Diamond, L.K.H. Leung et al., Conceptual mechanical design for a pressure-tube type supercritical water-cooled reactor. *Paper presented at the 5th International Symposium on Supercritical-Water-Cooled Reactors* (Vancouver, British Columbia, Canada, 13–16 March 2011)
4. D.L. Hetrick, *Dynamics of Nuclear Reactors*, (The University of Chicago Press, 1971)
5. G.R. Ansarifar, M. Rafiei, Higher-order sliding mode controller design for a research nuclear reactor considering the effect of xenon concentration during load following operation. *Ann. Nucl. Energy* **75**, 728–735 (2015). <https://doi.org/10.1016/j.anucene.2014.09.021>
6. P.W. Sun, B. Wang, J. Zhang et al., Control of Canadian once-through direct cycle supercritical water-cooled reactors. *Ann. Nucl. Energy* **81**, 6–17 (2015). <https://doi.org/10.1016/j.anucene.2015.03.008>
7. V. Utkin, Variable structure systems with sliding modes. *IEEE Trans. Automat.* **22**, 212–222 (1977). <https://doi.org/10.1109/TAC.1977.1101446>
8. G.R. Ansarifar, H. Davilu, H.A. Talebi, Gain scheduled dynamic sliding mode control for nuclear steam generators. *Prog. Nucl. Energy* **53**, 651–663 (2011). <https://doi.org/10.1016/j.pnucene.2011.04.029>
9. G.R. Ansarifar, H.R. Akhavan, Sliding mode control design for a PWR nuclear reactor using sliding mode observer during load following operation. *Ann. Nucl. Energy* **75**, 611–619 (2015). <https://doi.org/10.1016/j.anucene.2014.09.019>
10. L. Fridman, A. Levant, *Higher-order sliding modes*, (Chihuahua Institute of Technology, Chihuahua, Mexico, 2002)
11. K. Zare, H.R. Koofgar, Adaptive second order sliding mode controller for two-input two output uncertain nonlinear systems and application to a 2-DOF helicopter model. *Modares Mech. Eng.* **15**(12), 189–199 (2016)

Springer Nature or its licensor (e.g. a society or other partner) holds exclusive rights to this article under a publishing agreement with the author(s) or other rightsholder(s); author self-archiving of the accepted manuscript version of this article is solely governed by the terms of such publishing agreement and applicable law.